Uncertainty and Disturbance Estimator-Based Control of a Flapping Wing Aerial Vehicle with Unknown Backlash-like Hysteresis

Zhao Yin, Wei He, Okyay Kaynak, Chenguang Yang, Long Cheng, Yu Wang

Abstract — Robust and accurate control of a flapping-wing aerial vehicle (FWAV) system is a challenging problem due to the existence of backlash-like hysteresis nonlinearity. This paper proposes uncertainty and disturbance estimator (UDE)-based control with output feedback for FWAV systems. The approach enables the acquisition of the approximate plant model with only a partial knowledge of system parameters. For the design of the controller, only the bandwidth information of the unknown plant model is needed. which is available through the UDE filter. The stability analysis of the closed-loop system with the UDE-based controller is presented. It is shown that the proposed control scheme can ensure the boundedness of the control signals. A number of numerical simulations are carried out to demonstrate the satisfactory trajectory tracking performance of the proposed method.

Index Terms — Uncertainty and disturbance estimator (UDE); Flapping wing aerial vehicle (FWAV); Hysteresis; Backlash.

I. Introduction

In recent years, unmanned aerial vehicles (UAVs) have received significant attention from both engineers and researchers. In this wide research area, flapping-wing aerial vehicles (FWAVs) have received a special attention due to the features of small size and low energy consumption. [1]–[3]. There are a number of superiorities of an FWAV. For example, it can combine precise and highly maneuverable hovering with energy efficient forward flight, it can, with its high biomimetic, be used to drive away birds to avoid damage to crops, and it can be useful in military reconnaissance because of its convincing camouflage. Therefore, study of advanced FWAV technologies is very meaningful and timely [4], [5].

In this paper, we study the FWAV system with motor, which is the main drive mode. The hysteresis phenomenon is therefore unavoidable due to the presence of the gear sets. The design of a controller that will compensate the backlash hysteresis is therefore a necessary task to ensure the stability of the system. Backlash hysteresis is quite a common problem in many systems such as electromagnetism, mechanical actuators and gear systems [6]–[12]. It is caused by inertia, magnetism, or friction when the actuated motion direction is reversed, and often severely affects system performance in the form of inaccuracies, oscillations, and instabilities. Extensive studies can be seen in the literature that propose new models and new control approaches to compensate for backlash-like hysteresis in nonlinear systems. In [13], the authors propose adaptive neural network controllers for a 3-DOF robotic manipulator to solve the problem of backlash hysteresis with state feedback and output feedback. The authors present an adaptive output feedback controller for a class of nonlinear systems with unknown backlash-like hysteresis in [14] and verify that the control method proposed can compensate the influence of hysteresis. In [15], the Preisach model, a well-known model, is investigated to deal with problem of elastic robot joints with hysteresis and backlash. The hysteresis is considered as external factor, like a disturbance in [16], and a disturbance observer is used to estimate it, as a result of which a good compensation effect is obtained. This method is very succinct, it does not need to a reformulation of the plant model.

In most instances, some uncertain terms cannot be measured. In the FWAV system disturbance is also unknown. Therefore, there can be seen numerous control schemes and methods proposed in literature to estimate these uncertainties [17]–[26]. The use of a neural network in the controller is proposed in [27] to approximate the unknown terms, and it is demonstrated that the approach can result in a good approximation effect. An adaptive controller is designed in [28] to alleviate the problem of unknown system parameters, and a disturbance observer is used to compensate them. In an earlier work, a backstepping scheme is presented to design an effective controller for flexible joint robotic manipulators in [29]. In that paper, the authors apply an adaptive controller to compensate for system uncertainty and unknown but bounded disturbance. An adaptive fuzzy output feedback control law is designed in [30]. In [31], an uncertainty and disturbance estimator (UDE)-based robust power flow controller is developed for electrical power system to realize power delivery to the grid precisely. In [32], a strategy based on UDE is developed to solve the effect of hysteresis nonlinearity and improve the performance of the positioning control of the piezoelectric stage. The UDE-based control is a method, which

Z. Yin and W. He are with the School of Automation and Electrical Engineering, the Institute of Artificial Intelligence, University of Science and Technology Beijing, Beijing 10083, China. (Corresponding author: Wei He, Email: weihe@ieee.org).

O. Kaynak is with the School of Automation and Electrical Engineering, Institute of Artificial Intelligence, University of Science and Technology Beijing, Beijing 100083, China, and also with Bogazici University, Istanbul 34342, Turkey.

L. Cheng and Y. Wang are with the Institute of Automation, Chinese Academy of Sciences, Beijing 100190, China.

C. Yang is with Bristol Robotics Laboratory, University of the West of England, Bristol, BS16 1QY, UK.

This work was supported in part by the National Key Research and Development Program of China under Grant 2017YFB1300102 and Major Science and Technology Fund of Beijing under Grant Z181100003118006.

does not require the linear parameterizations and external interference information. Furthermore, the scheme has good robustness property with a straightforward structure. In recent years, more and more studies can be seen in literature that investigates the use of the UDE approach in different ways, such as in connection with a nonlinear system [33], sliding model control [34], electrical power system [31], piezoelectric stages [32], and so on [35]–[40]. Similar to these efforts, this article proposes a robust control strategy that is based on a UDE for FWAV systems to improve the performance in the presence of uncertainties and disturbance.

Regarding the UDE works, the novelty and the contribution of this paper lie in applying and validating the UDE-based control strategy to FWAV systems, which is a challenging problem. Moreover, for the first time in the literature, we have disclosed that the challenging problem of designing an output feedback controller using UDE can be converted into the design of a low-pass filter. Compared to those existing control methods, the main contributions of this paper are highlighted as follows:

(i) Hysteresis phenomenon is considered due to the presence of the gear sets in an FWAV that is driven by a motor;
(ii) UDE-based control law for FWAV systems with output feedback is derived to resolve the uncertain terms;
(iii) The proposed control method results in a good and robust performance, and the desired trajectory tracking is attained. Additionally comparative arguments are provided to obtain the best control parameters.

The rest of the paper is organized as follows: Section II covers the problem formulation and the preliminaries using some necessary lemmas, properties and assumptions. The UDE-based controller design with output feedback and stability analysis are illustrated in section III. Simulation studies are presented in Section IV. Section V concludes the paper.

II. Problem Formulation and Preliminaries

A. Problem Formulation

The dynamics of FWAV can be expressed as [5]:

$$\mathbf{M}(\mathbf{q})\ddot{\mathbf{q}} + \mathbf{C}(\mathbf{q},\dot{\mathbf{q}})\dot{\mathbf{q}} + \mathbf{G}(\mathbf{q}) = \mathbf{F}(\tau) \tag{1}$$

The terms of the above equation are defined as follows: $\mathbf{q} = [\mathbf{q_t} \quad \mathbf{q_r}]^T = [x \quad y \quad z \quad \alpha \quad \beta \quad \gamma]^T$, $\mathbf{M} = \begin{bmatrix} \mathbf{M_t} & \mathbf{0}_{3\times3} \\ \mathbf{0}_{3\times3} & \mathbf{M_r} \end{bmatrix}$, $\mathbf{C} = \begin{bmatrix} \mathbf{0}_{3\times3} & \mathbf{0}_{3\times3} \\ \mathbf{0}_{3\times3} & \mathbf{C_r} \end{bmatrix}$, $\mathbf{G} = \begin{bmatrix} \mathbf{G_t} \\ \mathbf{0}_{3\times1} \end{bmatrix}$, $\mathbf{F}(\tau) = \mathbf{R}(\mathbf{q})\phi(\tau) = \begin{bmatrix} \mathbf{R^{IB}}(\mathbf{q_r}) & \mathbf{0}_{3\times3} \\ \mathbf{0}_{3\times3} & \mathbf{I}_{3\times3} \end{bmatrix}\phi(\tau)$, where $\mathbf{q_t} = [x \quad y \quad z]^T$ is the position states in the inertial frame and $\mathbf{q_r} = [\alpha \quad \beta \quad \gamma]^T$ denotes the attitude angles of the body frame. $\mathbf{M_t} = m\mathbf{I}_{3\times3}$ is the mass matrix. $\mathbf{M_r} = \mathbf{I_p}\mathbf{T}$ and $\mathbf{C_r} = \mathbf{I_p}\dot{\mathbf{T}} + \mathbf{L}$, where $\mathbf{I_p}$ presents the moment of inertia matrix and $\mathbf{T} = \begin{bmatrix} 1 & 0 & -\sin(\beta) \\ 0 & \cos(\alpha) & \cos(\beta)\sin(\alpha) \\ 0 & -\sin(\alpha) & \cos(\beta)\cos(\alpha) \end{bmatrix}$. L is a square matrix and defined as: $(\mathbf{T}\dot{\mathbf{q}}_\mathbf{r}) \times \mathbf{I_p}(\mathbf{T}\dot{\mathbf{q}}_\mathbf{r}) = \mathbf{L}\dot{\mathbf{q}}_\mathbf{r}$, $\mathbf{G_t} = [0 \quad 0 \quad -mg]^T$ denotes the gravity vector. $\mathbf{F}(\tau)$ is input function, and $\phi(\tau)$ repsents the backlash hysteris input nonlinearity. $\mathbf{R^{IB}}(\mathbf{q_r}) = (\mathbf{R^{BI}}(\mathbf{q_r}))^{-1}$, where $\mathbf{R^{BI}} = \mathbf{C^{B2}}\mathbf{C^{21}}\mathbf{C^{1I}}$ is the rotation matrix, where

$$\mathbf{C^{B2}} = \begin{bmatrix} 1 & 0 & 0 \\ 0 & \cos(\alpha) & \sin(\alpha) \\ 0 & -\sin(\alpha) & \cos(\alpha) \end{bmatrix}$$

$$\mathbf{C^{21}} = \begin{bmatrix} \cos(\beta) & 0 & -\sin(\beta) \\ 0 & 1 & 0 \\ \sin(\beta) & 0 & \cos(\beta) \end{bmatrix}$$

$$\mathbf{C^{1I}} = \begin{bmatrix} \cos(\gamma) & \sin(\gamma) & 0 \\ -\sin(\gamma) & \cos(\gamma) & 0 \\ 0 & 0 & 1 \end{bmatrix}$$

The front view and side view of our FWAV model are shown in Fig. 1. The wing frame (X^W, Y^W, Z^W) is used to describe flapping, rotation and deviation angles associated with the stroke plane. (X^B, Y^B, Z^B) is the body frame.

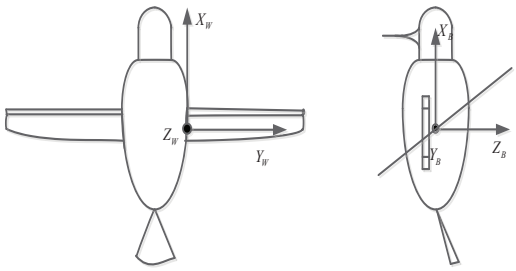

Fig. 1. Front and side view of FWAV model

The backlash hysteresis nonlinearity can be described by [41]:

$$\mu = \phi(\tau) = \begin{cases} h(\tau - B), & \dot{\tau}(t) > 0 \text{ and } \mu(t) = h(\tau(t) - B) \\ h(\tau + B), & \dot{\tau}(t) < 0 \text{ and } \mu(t) = h(\tau(t) + B) \\ \phi(t\_), & \text{otherwise} \end{cases} \tag{2}$$

where $\phi(\tau)$ denotes the backlash operator, h is the slope of the lines, B is the backlash distance and $\phi(t\_)$ means no change occurs in $\phi(\tau)$. However, this function is discontinuous and not applicable to a controller design that requires continuous signals. A continuous function to describe the backlash hysteresis is defined as [42]:

$$\frac{du_i}{dt} = \chi_i \left|\frac{d\tau_i}{dt}\right| [h_i\tau_i - u_i] + \kappa_i \frac{d\tau_i}{dt}, \quad i = 1, 2 \tag{3}$$

where χ, κ and h are constants and $h > \kappa$. The equation can be solved explicitly as

$$u_i(t) = h_i\tau_i(t) + d_i(\tau) \tag{4}$$

$$d_i(\tau_i) = [\mu_i(0) - h_i\tau_i(0)]e^{-\chi_i(\tau_i - \tau_i(0))\text{sgn}(\dot{\tau}_i)} + e^{-\chi_i\tau_i\text{sgn}(\dot{\tau}_i)} \int_{\tau_i(0)}^{\tau_i} [\beta_i - h_i]e^{-\chi_i\zeta\text{sgn}(\dot{\tau}_i)}d\zeta \tag{5}$$

The solution indicates that (3) can be used to model a class of backlash-like hysteresis ,where the parameters are $\chi_i = 1$, $h_i = 3.15$, $\kappa = 0.35$, $\tau(t) = x\sin(2.3t), x = 2.5, 3.5, 4.5$.

The backlash hysteresis input nonlinearity $\phi(\tau)$, can be written as

$$\phi(\tau) = \mathbf{H_a}\tau + \mathbf{D}(\tau) \tag{6}$$

where

$$\mathbf{H_a} = \mathrm{diag}\{h_1, h_2, \ldots, h_6\} > 0$$

and $\mathbf{D}(\tau) = [d_1(\tau_1), d_2(\tau_2), \ldots, d_6(\tau_6)]^T$ and $|d_i(\tau_i)| \leq d_i^*$ with $||\mathbf{D}(\tau)|| \leq D^* = \sqrt{d_1^{*2} + d_2^{*2} + \ldots + d_6^{*2}}$. The control objective is to design a stable UDE-based controller for the flapping wing robot so that it follows a desired trajectory. The following assumptions and lemma will help achieve our objective.

Assumption 1: [41] The desired trajectory is known, continuous and bounded.

Assumption 2: [43] The slopes of the backlash like hysteresis H_a is unknown, but there exists positive constants $\bar{h}_a^*$ and $\underline{h}_a^*$ such that $\underline{h}_a^* \leq \| \mathbf{H_a} \| \leq \bar{h}_a^*$ and $\|\mathbf{M}\| \leq m^*$.

Lemma 1: [44] A Lyapunov Function candidate $\mathbf{V}(\mathbf{x})$ is bounded if the inital condition $\mathbf{V}(\mathbf{x}(\mathbf{0}))$ is bounded, $\mathbf{V}(\mathbf{x})$ is positive definite and continuous and if

$$\dot{\mathbf{V}}(\mathbf{x}) \leq -\rho \mathbf{V}(\mathbf{x}) + \mathbf{C} \tag{7}$$

where $\rho > 0$ is a constant matrix, and $\mathbf{C} > 0$ a constant vector.

III. Controller Design

A UDE-based robust controller for an FWAV system is presented in this section. The control objective is to track the desired position and angle trajectories of the FWAV in the presence of backlash hysteresis. The scheme is basically a state feedback controller with UDE-based. It is assumed the state information of q and $\dot{q}$, and the actual trajectories are available. The case when the velocity information is not available is also considered, naming it as the output feedback control scheme, as shown in Fig. 2.

The dynamics of the FWAV can, by the use (1) and (6), be rewritten as

$$\ddot{\mathbf{q}} = \mathbf{M^{-1}}(\mathbf{q})[\mathbf{R}(\mathbf{q})(\mathbf{H_a}\tau + \mathbf{D}(\tau)) - \mathbf{C}(\mathbf{q}, \dot{\mathbf{q}})\dot{\mathbf{q}} - \mathbf{G}(\mathbf{q})] \tag{8}$$

The generalized tracking error variable $\mathbf{q_e}$ is defined as

$$\mathbf{q_e} = \mathbf{q} - \mathbf{q_d} \tag{9}$$

where $\mathbf{q_d}$ is the desired trajectory. Its time derivative is defined as

$$\dot{\mathbf{q}}_\mathbf{e} = \dot{\mathbf{q}} - \dot{\mathbf{q}}_\mathbf{d} \tag{10}$$

And the filtered error is defined as

$$\mathbf{q_z} = \dot{\mathbf{q}}_\mathbf{e} + \mathbf{\Lambda} \mathbf{q_e} \tag{11}$$

where $\mathbf{\Lambda} = \mathbf{\Lambda^T} > \mathbf{0}$. Then define the following stable linear reference model as

$$\ddot{\mathbf{q}}_\mathbf{d} = -\mathbf{A_d}\dot{\mathbf{q}}_\mathbf{d} - \mathbf{B_d}\mathbf{q_d} - \mathbf{C_d}\mathbf{c} \tag{12}$$

where $\mathbf{c} = [\mathbf{c_t}, \mathbf{c_r}]^T = [c_x, c_y, c_z, c_\alpha, c_\beta, c_\gamma]^T \in \mathbb{R}^6$ is a piecewise continuous and uniformly bounded command, $A_d \in \mathbb{R}^{6\times6}$, $B_d \in \mathbb{R}^{6\times6}$ and $C_d \in \mathbb{R}^{6\times6}$ are selected to satisfy the ideal specification of the closed-loop system.

In this paper, the desired error dynamics about $\mathbf{q_e}$ is

$$\dot{\mathbf{q}}_\mathbf{z} = -\mathbf{K}\mathbf{q_e} \tag{13}$$

where $\mathbf{K} = \mathbf{K^T} > \mathbf{0}$ denotes the error feedback gain.

According to (8), (11), (12) and (13), we can obtain that

$$\begin{aligned} &\mathbf{M}^{-1}[\mathbf{R}(\mathbf{q})(\mathbf{H_a}\tau + \mathbf{D}(\tau)) - \mathbf{C}(\mathbf{q}, \dot{\mathbf{q}})\dot{\mathbf{q}} \\ &-\mathbf{G}(\mathbf{q})] + \mathbf{A_d}\dot{\mathbf{q}}_\mathbf{d} + \mathbf{B_d}\mathbf{q_d} + \mathbf{C_d}\mathbf{c} \\ =\ &-(\mathbf{K} + \mathbf{\Lambda})\dot{\mathbf{q}}_\mathbf{e} - \mathbf{K}\mathbf{\Lambda}\mathbf{q_e} \end{aligned} \tag{14}$$

Then these uncertain terms can be denoted and rewritten as a new dynamic equation

$$\begin{aligned} &-(\mathbf{K} + \mathbf{\Lambda})\dot{\mathbf{q}}_\mathbf{e} - \mathbf{K}\mathbf{\Lambda}\mathbf{q_e} \\ =\ &\mathbf{A_d}\dot{\mathbf{q}}_\mathbf{d} + \mathbf{B_d}\mathbf{q_d} + \mathbf{C_d}\mathbf{c} + \mathbf{u_d} + b\tau \end{aligned} \tag{15}$$

where

$$\begin{aligned} \mathbf{u_d} = \mathbf{M^{-1}}(\mathbf{x})[&\mathbf{R}(\mathbf{q})(\mathbf{H_a}\tau + \mathbf{D}(\tau)) \\ &-\mathbf{C}(\mathbf{q}, \dot{\mathbf{q}})\dot{\mathbf{q}} - \mathbf{G}(\mathbf{q})] - b\tau \end{aligned} \tag{16}$$

Then through the transpose, there is

$$\begin{aligned} b\tau =\ &-(\mathbf{K} + \mathbf{\Lambda})\dot{\mathbf{q}}_\mathbf{e} - \mathbf{K}\mathbf{\Lambda}\mathbf{q_e} \\ &-\mathbf{A_d}\dot{\mathbf{q}}_\mathbf{d} - \mathbf{B_d}\mathbf{q_d} - \mathbf{C_d}\mathbf{c} - \mathbf{u_d} \end{aligned} \tag{17}$$

where b is an equivalent control parameter associated with the control performance, then the uncertain terms can be obtained as $\mathbf{u_d} = \ddot{\mathbf{q}} - b\tau$, which denotes the uncertainties can be derived from the known part of dynamics and control signal. We can know that they cannot be used to design a controller straightly. Therefore, assume that the frequency range of a signal is restricted, and the signal can be approximated by using a filter with the proper bandwidth, then the process of UDE-based control is designed in [35], which is presented to handle the problem of system uncertainty. Meanwhile, assume that $G_f(s)$ is a proper stable filter with the gain and zero phase shift over the spectrum of $\mathbf{u_d}$ and zero gain elsewhere. Then, the uncertain terms $\mathbf{u_d}$ can be approximated as

$$\hat{\mathbf{u}}_\mathbf{d} = \mathcal{L}^{-1}\{G_f(s)\} * \mathbf{u_d} = \mathcal{L}^{-1}\{G_f(s)\} * (\ddot{\mathbf{q}} - b\tau) \tag{18}$$

where $\hat{\mathbf{u}}_\mathbf{d}$ is an estimate term of $\mathbf{u_d}$, " $*$ " represents the convolution operation, and $\mathcal{L}^{-1}\{\cdot\}$ denotes the inverse Laplace transform of " $\cdot$ ".

Remark 1: The theoretical principle of the filter selection is that, the filter $G_f(s)$ should be designed with the unity gain and zero phase shift over the spectrum of u_d and zero gain elsewhere [35]. In [36], [45], the authors offer the detailed guideline of the filter selection. However, the parameters of filter cannot be selected too small because of the hardware limitations in practice. In addition, the sensor noise with high frequency would be caused by the filter with too wide bandwidth, and it might degrade the performance of the UDE-based controller. Thus, how to choose a proper filter depends on the specific application including the hardware capability and the practical necessity.

Replacing $\mathbf{u_d}$ with $\hat{\mathbf{u}}_\mathbf{d}$ in (17) results in

$$\begin{aligned} b\tau =\ &-(\mathbf{K} + \mathbf{\Lambda})\dot{\mathbf{q}}_\mathbf{e} - \mathbf{K}\mathbf{\Lambda}\mathbf{q_e} - \mathbf{A_d}\dot{\mathbf{q}}_\mathbf{d} - \mathbf{B_d}\mathbf{q_d} - \mathbf{C_d}\mathbf{c} \\ &-\mathcal{L}^{-1}\{G_f(s)\} * (\ddot{\mathbf{q}} - b\tau) \end{aligned} \tag{19}$$

Furthermore, the UDE-based controller can be obtained from

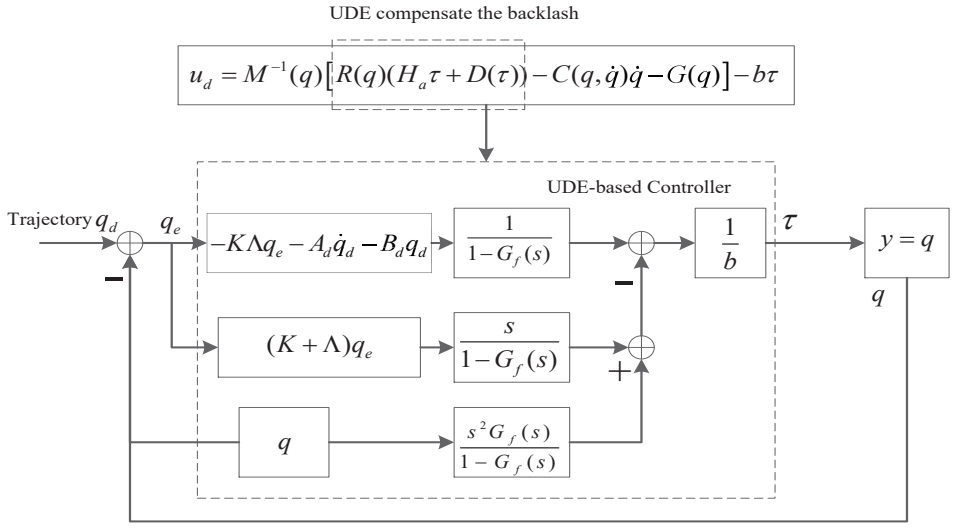

Fig. 2. The proposed UDE-based control strategy with output-feedback

(19) as

$$\begin{aligned}\tau = \frac{1}{b}\Big\{&\mathcal{L}^{-1}\Big\{\frac{1}{1-G_f(s)}\Big\} * (-(\mathbf{K}+\mathbf{\Lambda})\dot{\mathbf{q}}_\mathbf{e} \\ &-\mathbf{K\Lambda q_e} - \mathbf{A_d}\dot{\mathbf{q}}_\mathbf{d} - \mathbf{B_d q_d} - \mathbf{C_d c}) \\ &-\mathcal{L}^{-1}\Big\{\frac{sG_f(s)}{1-G_f(s)}\Big\} * \dot{\mathbf{q}}\Big\}\end{aligned} \tag{20}$$

Since the above controller (20) requires full states $\mathbf{q}$, and $\dot{\mathbf{q}}$ to be measured. However, some state information cannot be obtained in the absence of velocity sensors. In that situation, an output feedback control law can be derived from (20) as

$$\begin{aligned}\tau = \frac{1}{b}\Big\{&\mathcal{L}^{-1}\Big\{\frac{1}{1-G_f(s)}\Big\} * (-\mathbf{K\Lambda q_e} - \mathbf{A_d}\dot{\mathbf{q}}_\mathbf{d} - \mathbf{B_d q_d} \\ &-\mathbf{C_d c}) - \mathcal{L}^{-1}\Big\{\frac{s}{1-G_f(s)}\Big\} * (\mathbf{K}+\mathbf{\Lambda q_e}) \\ &-\mathcal{L}^{-1}\Big\{\frac{s^2 G_f(s)}{1-G_f(s)}\Big\} * \mathbf{q}\Big\}\end{aligned} \tag{21}$$

Obviously, the degree of the filter $G_f(s)$ in (21) should not be less than 2 to guarantee the structure of control be realized, i.e., $[s^2 G_f(s)]/[1-G_f(s)]$ should be suitable.

Consider the following Lyapunov candidate function

$$\mathbf{V_1} = \frac{1}{2}\mathbf{q_z^T q_z} \tag{22}$$

Differentiating (22) with respect to time, along with (11) and (17) yields,

$$\begin{aligned}\dot{\mathbf{V}}_\mathbf{1} &= \mathbf{q_z^T}\dot{\mathbf{q}}_\mathbf{z} \\ &= \mathbf{q_z^T}(\ddot{\mathbf{q}}_\mathbf{e} + \mathbf{\Lambda}\dot{\mathbf{q}}_\mathbf{e}) \\ &= \mathbf{q_z^T}(\mathbf{u_d} + \mathbf{b}\tau - \ddot{\mathbf{q}}_\mathbf{d} + \mathbf{\Lambda}\dot{\mathbf{q}}_\mathbf{e})\end{aligned} \tag{23}$$

with the UDE-based controller (21), and substituting (19) into (23), we can obtain

$$\begin{aligned}\dot{\mathbf{V}}_1 &= \mathbf{q_z^T}(-\mathbf{K q_z} + \mathbf{u_d} - \hat{\mathbf{u}}_\mathbf{d}) \\ &= -\mathbf{q_z^T K q_z} - \mathbf{q_z^T}\tilde{\mathbf{u}}\end{aligned} \tag{24}$$

where $\tilde{\mathbf{u}}_\mathbf{d} = \mathbf{u_d} - \hat{\mathbf{u}}_\mathbf{d}$ is the estimated error of the uncertainty terms, in the accordance with the (18), the estimated error can be proposed as

$$\tilde{\mathbf{u}}_\mathbf{d} = \mathbf{u_d} * \mathcal{L}^{-1}\{1 - G_f(s)\} \tag{25}$$

Since we assume that $G_f(s)$ is a strictly suitable stable filter with proper bandwidth. Then, we can obtain

$$\begin{aligned}\dot{\mathbf{V}}_\mathbf{1} &\leq -\mathbf{q_z^T K q_z} + \frac{1}{2}\mathbf{q_z^T q_z} + \frac{1}{2}\tilde{\mathbf{u}}^\mathbf{2} \\ &\leq -\mathbf{q_z^T}(\mathbf{K} - \frac{1}{2}\mathbf{I})\mathbf{q_z} + \frac{1}{2}\tilde{\mathbf{u}}^\mathbf{2} \\ &\leq -\rho\mathbf{V_1} + \mathbf{C_1}\end{aligned} \tag{26}$$

where $\rho_\mathbf{1}$ and $\mathbf{C_1}$ are define as

$$\rho_\mathbf{1} = \min\{2(\mathbf{K} - \frac{1}{2}\mathbf{I})\} \tag{27}$$

$$\mathbf{C_1} = \frac{1}{2}\tilde{\mathbf{u}}^2 \tag{28}$$

Proof: Multiplying (26) by $\mathbf{q_e^{\rho_1} t}$, we have

$$\frac{d}{dt}(\mathbf{V_1 e^{\rho_1 t}}) \leq \mathbf{C_1 e^{\rho_1 t}} \tag{29}$$

By integrating the equation and according to (22), we have

$$\frac{1}{2}\|\mathbf{q_z}\|^2 \leq \mathbf{V_1}(\mathbf{q}(0)) + \frac{\mathbf{C_1}}{\rho_\mathbf{1}} \tag{30}$$

It is clear that $\|\mathbf{q_e}\|$ can be reduced by increasing the control parameter $\mathbf{K}$ and designing the filter $G_f(s)$ to reduce the estimation error $\tilde{\mathbf{u}}$. if the estimation error $\tilde{\mathbf{u}}$ converges to zero, then the error signal $\mathbf{q_e}$ converges to zero too. According to the claim that the filter $G_f(s)$ is designed as a strictly proper stable filter in [35], we can obtain that $\|\tilde{\mathbf{u}}\| \approx 0$. Therefore, the error signal $\mathbf{q_e}$ is uniformly bounded according to Lemma 1. ■

Hence, we can obtain that z converges to a compact which is semiglobal uniformly bounded. Due to $\mathbf{q_z} = \dot{\mathbf{q}}_\mathbf{e} + \mathbf{\Lambda q_e}$, that is, $\dot{\mathbf{q}}_\mathbf{e} = -\mathbf{\Lambda q_e} + \mathbf{q_z}$, using the same proof method we can obtain that $\mathbf{q_e} \leq \mathbf{q_e}(\mathbf{q}(0)) + \frac{\mathbf{q_z}}{\mathbf{\Lambda}}$.

IV. Numerical Simulations

In this part, simulations are implemented to verify our proposed controllers. The parameters of FWMAV model are listed in Table I.

TABLE I
PARAMETERS OF THE FWAV SYSTEM

Parameter	Description	Value
m	Total mass of the model	5.60g
w	Body width	24mm
l_1	Body length	77.5mm
l_2	Wing length	53mm
I_{xx}	Moment of inertia	575gmm^2
I_{yy}	Moment of inertia	576gmm^2
I_{zz}	Moment of inertia	991gmm^2

Comparing the system with the plat model in (8), the reference model is chosen as

$$\ddot{q}_d = -A_d\dot{q}_d - B_d q_d - C_d c \tag{31}$$

where $A_d = \text{diag}[200, 200, 200, 500, 500, 500]$, $B_d = \text{diag}[500, 500, 500, 800, 800, 800]$, and $C_d = \text{diag}[100, 100, 100, 200, 200, 200]$. The desired position $\mathbf{c_t}$ of FWAV can be chosen as

$$\begin{cases} c_x(t) = 100\sin(\pi t) \\ c_y(t) = 100\sin(\pi t) \\ c_z(t) = 100\sin(\pi t) \end{cases} \tag{32}$$

and the desired attitude $\mathbf{c_r}$ of FWAV are chosen as

$$\begin{cases} c_\alpha(t) = 2\sin(2t) \\ c_\beta(t) = 2\sin(2t) \\ c_\gamma(t) = 2\sin(2t) \end{cases} \tag{33}$$

The initial conditions for all states are given as $\mathbf{q}(0) = [10, 10, 10, 0.5, 0.5, 0.5]^T$, $\dot{\mathbf{q}}(0) = [0.01, 0.01, 0.01, 0.01, 0.01, 0.01]^T$. In the next several subsections, some tables are drawn to denote the tracking performance by using different kinds errors, such as Root Mean Square Error (RMSE) and Mean Absolute Error (MAE). And the detail formula expression of these errors are as follows:

$$RMSE = \sqrt{\frac{1}{N}\sum_{i=1}^{N}(Y_i - Y_{id})^2} \tag{34}$$

$$MAE = \frac{1}{N}\sum_{i=1}^{N}\|Y_i - Y_{id}\| \tag{35}$$

where Y_{id} denotes the reference value, and Y_i as the actual value.

A. Comparison with different controllers

In this section, we compare our output feedback controller (21) with PD controller and DOB-based controller. The PD controller is designed with $\tau_{\mathbf{pd}} = -\mathbf{K_p}\mathbf{e} - \mathbf{K_d}\dot{\mathbf{e}}$, where $\mathbf{K_p} = \text{diag}[200, 200, 200, 500, 500, 500]$, $\mathbf{K_d} = \text{diag}[500, 500, 500, 500, 500, 500]$. Other simulation parameters are selected as $b = 2$, $\mathbf{K} = [500, 500, 500, 800, 800, 800]$. In this case, we choose a second-order low-pass filter $G_f(s) = 1/[(Ts)^2 + \sqrt{2}Ts + 1]$, and T is selected as a small positive value to guarantee that the bandwidth covers the frequency spectrum of u_d. Consequently we choose $T = 0.01$. Especially, the internal-model-embeded DOB is considered for comparison, and for fair comparison, the filter is chosen the same as UDE control which is also a second-order filter. Then, the different errors which reflect the different tracking performance are shown in TABLE II. From TABLE II, we can see that there are three different controllers in total, and every controller branches off into two different errors that the first column denotes RMSE, and the second column shows MAE, respectively. From this table, we can conclude that all kinds of errors of the PD controllers is the greatest and the UDE-based controller is the smallest.

Furthermore, in order to make the data that in the table more intuitive and visible. We select two rows of data (the third row and the sixth row) to have a draw for comparison from the position and angle information in the table respectively. It can be seen from Fig. 3 and 4 that the errors converge to a small value close to zero. And we can obtain that the tracking line can track the desired trajectory indirectly. However, it is clear that the errors are smaller with the controllers proposed in this paper, compared with the PD control. In addition, we can also state from Fig. 3 and 4 that the DOB-based control performance is not good with a violent oscillation at the beginning of the tracking process. This is not easy to realise it in practice. Therefore, it can be concluded that the control approach suggested in this article is a more preferable one in tracking performance than other controllers. Furthermore, the DOB also needs a larger control effort compared to the UDE.

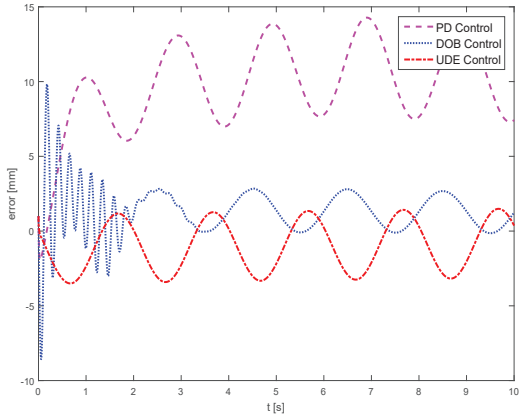

Fig. 3. Comparison of errors of position with different controllers (The data z in the third row of the TABLE II).

B. Comparison with compensation effect

In this section, we compare our output-feedback controller (21) with the controller without backlash hysteresis compensation. The simulation parameters are selected to be the same as in the last section.

The comparison of different errors of output-feedback controllers with compensation and without compensation are

TABLE II
THE DIFFERENT ERRORS OF STATES OF THE FWAV SYSTEM WITH DIFFERENT CONTROLLERS

	PD Control		DOB Control		UDE Control	
x	3.0220	2.5383	1.7654	1.2604	1.9491	1.6408
y	5.3401	4.7160	1.6265	1.1903	1.9493	1.6408
z	10.1548	9.7324	2.1196	1.5851	1.9366	1.6337
α	0.3905	0.3383	0.0353	0.0260	0.0220	0.0188
β	0.3378	0.2918	0.0325	0.0242	0.0189	0.0157
γ	0.4435	0.3816	0.0604	0.0464	0.0240	0.0199

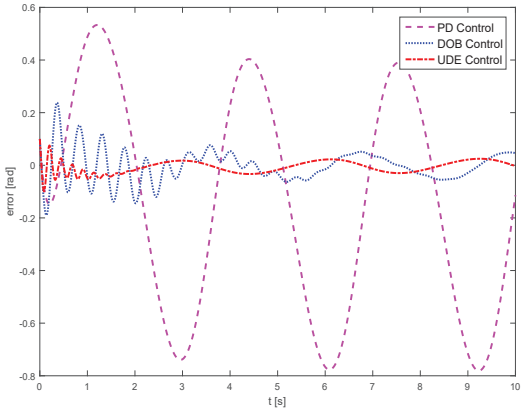

Fig. 4. Comparison of errors of attitude with different controllers (The data γ in the sixth row of the TABLE II).

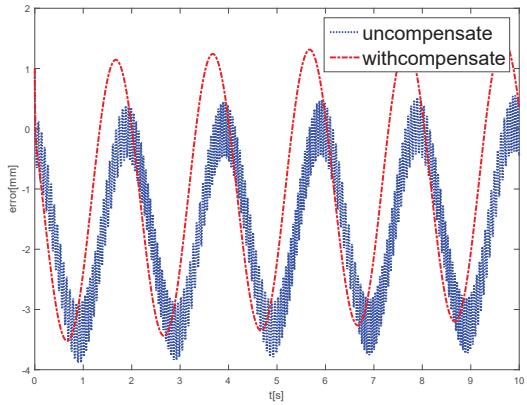

Fig. 5. Comparison of errors of position with compensation and uncompensation. (The data x in the first row of the TABLE III).

shown in the TABLE III. It is the same as the last section, the first subcolumn denotes RMSE, and the second subcolumn shows MAE. It is obvious that all the numbers of errors of the controller without backlash hysteresis compensation are larger than the controller with compensation from these data. Moreover, in order to make the data that in the table more intuitive and visible. We select two rows of data (the first row and the fourth row) to have a draw for comparison from the position and angle information in the table respectively like IV-A. It can be seen from Fig. 5 and 6 that the errors of the controllers with compensation are less than the without one, and the error line is very unsmooth with high-frequency spikes for the controller without compensation. Therefore, we can see that the control approach proposed in this paper is more viable to solve the backlash problem, and that it is necessary to consider the compensation of backlash hysteresis.

TABLE III
THE DIFFERENT ERRORS OF STATES OF THE FWAV SYSTEM WITH BACKLASH COMPENSATION OR NOT

	With Compensation		Without Compensation	
x	1.9491	1.6408	2.0673	1.7067
y	1.9493	1.6408	2.0674	1.7075
z	1.9366	1.6337	2.0496	1.6887
α	0.0220	0.0188	0.0591	0.0502
β	0.0189	0.0157	0.0520	0.0462
γ	0.0240	0.0199	0.0651	0.0573

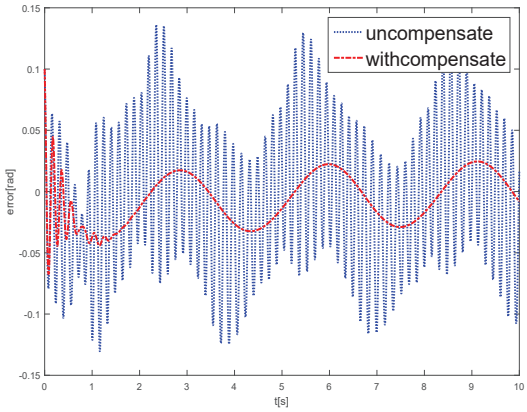

Fig. 6. Comparison of errors of attitude with compensation and uncompensation. (The data α in the fourth row of the TABLE III).

C. Comparison with different frequencies

In this section, we compare our output feedback control performance (21) with different frequencies. The simulation parameters are selected the same as section IV-A. Furthermore, the filter parameter T is adjusted as 0.01, 0.1, 1, respectively, and the corresponding cut-off frequency is 15.91Hz, 1.591Hz, 0.1591Hz.

The comparison of different errors of controller with different frequencies with output-feedback are shown in the TABLE IV. From this table, it can be observed that the all kinds errors of controller are reduced by choosing a larger bandwidth. The more distinct consequences can be seen in the Fig. 7 and 8 which is selected from TABLE IV (the first row

and the fourth row), it is obvious that the errors are smaller and smoother when a higher frequency is selected. From these two figures, another important conclusion we can derive is that when the frequency is chosen as 15.91Hz, the tracking errors are remarkably smaller than 1.591Hz and 0.1591Hz. This is a reasonable phenomenon after consulting the literature, and in practice 15.91Hz is a logical frequency for experiment.

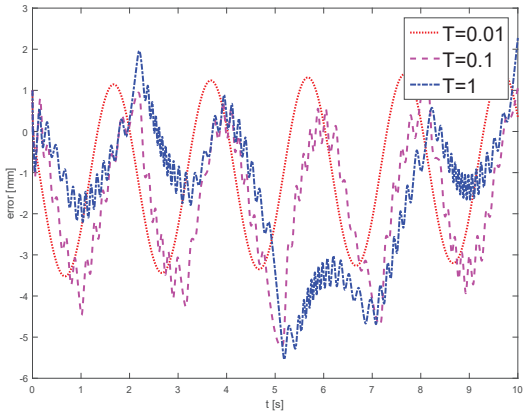

Fig. 7. Comparison of errors of position with different frequencies (The data x in the first row of the TABLE IV).

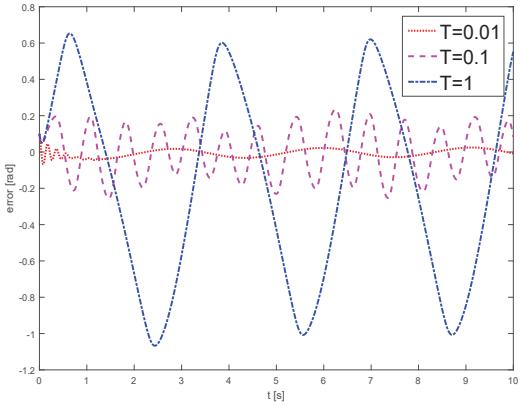

Fig. 8. Comparison of errors of attitude with different frequencies (The data α in the fourth row of the TABLE IV).

V. Conclusion

In this paper, we propose the UDE-based control for FWAV systems with backlash-like hysteresis. The output-feedback controller is presented in the controller design part. The UDE-based control is used to estimate the model uncertainty and to compensate the unknown hysteresis. Its main advantage is that the controller design does not require any knowledge of the uncertainty and the disturbance, except the information about their bandwidth. Extensive simulation results are presented, through which the validity of the proposed approach is verified. It is seen that the trajectory tracking performance is excellent. A number of comparative studies with different control methods are then presented, as well as with different cut-off frequencies, and whether backlash hysteresis compensation is used or not. By a thorough analysis of the simulation results, a number of deductions are arrived at. As future work, experimental implementation of the UDE-based control method is considered, as well as the use of the approach in other fields.

References

[1] A. A. Paranjape, S.-J. Chung, and J. Kim, "Novel dihedral-based control of flapping-wing aircraft with application to perching," *IEEE Transactions on Robotics*, vol. 29, no. 5, pp. 1071–1084, 2013.

[2] H. E. Taha, M. R. Hajj, and A. H. Nayfeh, "Flight dynamics and control of flapping-wing mavs: a review," *Nonlinear Dynamics*, vol. 70, no. 2, pp. 907–939, 2012.

[3] C. T. Orlowski and A. R. Girard, "Dynamics, stability, and control analyses of flapping wing micro-air vehicles," *Progress in Aerospace Sciences*, vol. 51, pp. 18–30, 2012.

[4] K. Y. Ma, P. Chirarattananon, S. B. Fuller, and R. J. Wood, "Controlled flight of a biologically inspired, insect-scale robot," *Science*, vol. 340, no. 6132, pp. 603–607, 2013.

[5] A. Banazadeh and N. Taymourtash, "Adaptive attitude and position control of an insect-like flapping wing air vehicle," *Nonlinear Dynamics*, vol. 85, no. 1, pp. 47–66, 2016.

[6] G.-Y. Gu, L.-M. Zhu, and C.-Y. Su, "Modeling and compensation of asymmetric hysteresis nonlinearity for piezoceramic actuators with a modified prandtl–ishlinskii model," *IEEE Transactions on Industrial Electronics*, vol. 61, no. 3, pp. 1583–1595, 2014.

[7] S. Rosenbaum, M. Ruderman, T. Strohla, and T. Bertram, "Use of jiles–atherton and preisach hysteresis models for inverse feed-forward control," *IEEE Transactions on Magnetics*, vol. 46, no. 12, pp. 3984–3989, 2010.

[8] R. Guruganesh, B. Bandyopadhyay, and H. Arya, "Robust stabilization of micro aerial vehicles with uncertain actuator nonlinearities," *International Journal of Micro Air Vehicles*, vol. 6, no. 1, pp. 43–62, 2014.

[9] J. Zhou, C. Wen, and Y. Zhang, "Adaptive backstepping control of a class of uncertain nonlinear systems with unknown backlash-like hysteresis," *IEEE Transactions on Automatic Control*, vol. 49, no. 10, pp. 1751–1759, 2004.

[10] X. Liu, C.-Y. Su, Z. Li, and F. Yang, "Adaptive neural-network-based active control of regenerative chatter in micromilling," *IEEE Transactions on Automation Science and Engineering*, vol. 15, no. 2, pp. 628–640, 2018.

[11] X. Chen, Y. Feng, and C.-Y. Su, "Adaptive control for continuous-time systems with actuator and sensor hysteresis," *Automatica*, vol. 64, pp. 196–207, 2016.

[12] W. He, W. Ge, Y. Li, Y.-J. Liu, C. Yang, and C. Sun, "Model identification and control design for a humanoid robot," *IEEE Transactions on Systems, Man, and Cybernetics: Systems*, vol. 47, no. 1, pp. 45–57, 2017.

[13] W. He, D. O. Amoateng, C. Yang, and D. Gong, "Adaptive neural network control of a robotic manipulator with unknown backlash-like hysteresis," *IET Control Theory & Applications*, vol. 11, no. 4, pp. 567–575, 2016.

[14] Y. Liu and Y. Lin, "Global adaptive output feedback tracking for a class of non-linear systems with unknown backlash-like hysteresis," *IET Control Theory & Applications*, vol. 8, no. 11, pp. 927–936, 2014.

[15] M. Ruderman, F. Hoffmann, and T. Bertram, "Modeling and identification of elastic robot joints with hysteresis and backlash," *IEEE Transactions on Industrial Electronics*, vol. 56, no. 10, pp. 3840–3847, 2009.

[16] J. Yi, S. Chang, and Y. Shen, "Disturbance-observer-based hysteresis compensation for piezoelectric actuators," *IEEE/ASME Transactions on Mechatronics*, vol. 14, no. 4, pp. 456–464, 2009.

[17] G. Wu, J. Sun, and J. Chen, "Optimal linear quadratic regulator of switched systems," *IEEE Transactions on Automatic Control*, 2018, In Press, DOI: 10.1109/TAC.2018.2872204.

[18] W. He, S. S. Ge, Y. Li, E. Chew, and Y. S. Ng, "Neural network control of a rehabilitation robot by state and output feedback," *Journal of Intelligent & Robotic Systems*, vol. 80, no. 1, pp. 15–31, 2015.

[19] D. Liu, Y. Xu, Q. Wei, and X. Liu, "Residential energy scheduling for variable weather solar energy based on adaptive dynamic programming," *IEEE/CAA Journal of Automatica Sinica*, vol. 5, no. 1, pp. 36–46, 2018.

[20] X. Chen and C.-Y. Su, "Adaptive control for ionic polymer-metal composite actuators," *IEEE Transactions on Systems, Man, and Cybernetics: Systems*, vol. 46, no. 10, pp. 1468–1477, 2016.

[21] X. Chen, C.-Y. Su, Z. Li, and F. Yang, "Design of implementable adaptive control for micro/nano positioning system driven by piezoelectric actuator," *IEEE Transactions on Industrial Electronics*, vol. 63, no. 10, pp. 6471–6481, 2016.

TABLE IV
THE DIFFERENT ERRORS OF STATES OF THE FWAV SYSTEM WITH DIFFERENT FREQUENCIES

	T = 0.01		T = 0.1		T = 1	
x	1.9491	1.6408	2.3179	1.8531	2.4622	1.9106
y	1.9493	1.6408	2.3572	1.9231	2.5436	2.0162
z	1.9366	1.6337	2.1316	1.7395	2.9679	1.8657
α	0.0220	0.0188	0.1357	0.1202	0.5687	0.4848
β	0.0189	0.0157	0.1324	0.1166	0.4573	0.3928
γ	0.0240	0.0199	0.1954	0.1696	0.8047	0.6835

[22] Y. Li and S. S. Ge, "Human–robot collaboration based on motion intention estimation," *IEEE/ASME Transactions on Mechatronics*, vol. 19, no. 3, pp. 1007–1014, 2014.

[23] W. He, S. S. Ge, and D. Huang, "Modeling and vibration control for a nonlinear moving string with output constraint," *IEEE/ASME Transactions on Mechatronics*, vol. 20, no. 4, pp. 1886–1897, 2015.

[24] C. Yang, Y. Jiang, Z. Li, W. He, and C.-Y. Su, "Neural control of bimanual robots with guaranteed global stability and motion precision," *IEEE Transactions on Industrial Informatics*, vol. 13, no. 3, pp. 1162–1171, 2017.

[25] C. Yang, C. Zeng, P. Liang, Z. Li, R. Li, and C.-Y. Su, "Interface design of a physical human–robot interaction system for human impedance adaptive skill transfer," *IEEE Transactions on Automation Science and Engineering*, vol. 15, no. 1, pp. 329–340, 2018.

[26] C. L. P. Chen, T. Zhang, L. Chen, and S. C. Tam, "I-ching divination evolutionary algorithm and its convergence analysis," *IEEE Transactions on Cybernetics*, vol. 47, no. 1, pp. 2–13, 2017.

[27] Z. Yin, W. He, and C. Yang, "Tracking control of a marine surface vessel with full-state constraints," *International Journal of Systems Science*, vol. 48, no. 3, pp. 535–546, 2017.

[28] X. He, W. He, J. Shi, and C. Sun, "Boundary vibration control of variable length crane systems in two-dimensional space with output constraints," *IEEE/ASME Transactions on Mechatronics*, vol. 22, no. 5, pp. 1952–1962, 2017.

[29] M. Bridges, D. M. Dawson, and C. Abdallah, "Contril of rigid-link, flexible-joint robots: a survey of backstepping approaches," *Journal of Field Robotics*, vol. 12, no. 3, pp. 199–216, 1995.

[30] Y. Li, S. Sui, and S. Tong, "Adaptive fuzzy control design for stochastic nonlinear switched systems with arbitrary switchings and unmodeled dynamics," *IEEE Transactions on Cybernetics*, vol. 47, no. 2, pp. 403–414, 2017.

[31] Y. Wang, B. Ren, and Q.-C. Zhong, "Robust power flow control of grid-connected inverters," *IEEE Transactions on Industrial Electronics*, vol. 63, no. 11, pp. 6887–6897, 2016.

[32] J. Chen, B. Ren, and Q.-C. Zhong, "Ude-based trajectory tracking control of piezoelectric stages," *IEEE Transactions on Industrial Electronics*, vol. 63, no. 10, pp. 6450–6459, 2016.

[33] B. Ren, Q.-C. Zhong, and J. Chen, "Robust control for a class of nonaffine nonlinear systems based on the uncertainty and disturbance estimator," *IEEE Transactions on Industrial Electronics*, vol. 62, no. 9, pp. 5881–5888, 2015.

[34] T. Chandrasekhar and L. Dewan, "Sliding mode control based on tdc and ude," *International Journal of Informatics and Systems Sciences*, vol. 3, no. 1, pp. 36–53, 2007.

[35] Q.-C. Zhong and D. Rees, "Control of uncertain lti systems based on an uncertainty and disturbance estimator," *Journal of dynamic systems, measurement, and control*, vol. 126, no. 4, pp. 905–910, 2004.

[36] B. Ren, Q.-C. Zhong, and J. Dai, "Asymptotic reference tracking and disturbance rejection of ude-based robust control," *IEEE Transactions on Industrial Electronics*, vol. 64, no. 4, pp. 3166–3176, 2017.

[37] S. Su and Y. Lin, "Robust output tracking control for a velocity-sensorless vertical take-off and landing aircraft with input disturbances and unmatched uncertainties," *International Journal of Robust and Nonlinear Control*, vol. 23, no. 11, pp. 1198–1213, 2013.

[38] B. Ren, Y. Wang, and Q.-C. Zhong, "Ude-based control of variable-speed wind turbine systems," *International Journal of Control*, vol. 90, no. 1, pp. 121–136, 2017.

[39] Y. Zhang, J. Sun, H. Liang, and H. Li, "Event-triggered adaptive tracking control for multiagent systems with unknown disturbances," *IEEE Transactions on Cybernetics*, 2018, In Press, DOI: 10.1109/TCYB.2018.2869084.

[40] Y. Dong and B. Ren, "Ude-based variable impedance control of uncertain robot systems," *IEEE Transactions on Systems, Man, and Cybernetics: Systems*, 2017, In Press, DOI: 10.1109/TSMC.2017.2767566.

[41] R.-J. Wai, Y.-C. Huang, Z.-W. Yang, and C.-Y. Shih, "Adaptive fuzzy-neural-network velocity sensorless control for robot manipulator position tracking," *IET Control Theory & Applications*, vol. 4, no. 6, pp. 1079–1093, 2010.

[42] C.-Y. Su, Y. Stepanenko, J. Svoboda, and T.-P. Leung, "Robust adaptive control of a class of nonlinear systems with unknown backlash-like hysteresis," *IEEE Transactions on Automatic Control*, vol. 45, no. 12, pp. 2427–2432, 2000.

[43] W.-D. Zhou, C.-Y. Liao, L. Zheng, and M.-M. Liu, "Adaptive fuzzy output feedback control for a class of nonaffine nonlinear systems with unknown dead-zone input," *Nonlinear Dynamics*, pp. 1–13, 2014.

[44] S. S. Ge and C. Wang, "Adaptive neural control of uncertain mimo nonlinear systems," *IEEE Transactions on Neural Networks*, vol. 15, no. 3, pp. 674–692, 2004.

[45] Q.-C. Zhong, A. Kuperman, and R. Stobart, "Design of ude-based controllers from their two-degree-of-freedom nature," *International Journal of Robust and Nonlinear Control*, vol. 21, no. 17, pp. 1994–2008, 2011.

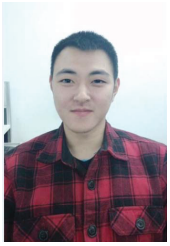

Zhao Yin (S'14) received his B.Eng. degree in electric engineering and automation from Hangzhou Dianzi University, Zhejiang, China, in 2013, and his M.Eng. degree in Control engineering from the School of Automation Engineering, University of Electronic Science and Technology of China, Chengdu, China, in 2016. He is currently pursuing the Ph. D. degree in control science and engineering with the School of Automation and Electrical engineering, University of Science and Technology Beijing, Beijing, China. His current research interests include control of flapping wing aerial vehicle, adaptive control, and multiple agent control.

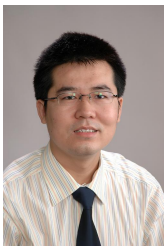

Wei He (S'09-M'12-SM'16) received his B.Eng. in automation and his M.Eng. degrees in control science and engineering from College of Automation Science and Engineering, South China University of Technology (SCUT), China, in 2006 and 2008, respectively, and his Ph.D. degree in control science and engineering from from Department of Electrical & Computer Engineering, the National University of Singapore (NUS), Singapore, in 2011.

He is currently working as a full professor in School of Automation and Electrical Engineering, University of Science and Technology Beijing, Beijing, China. He has co-authored 2 books published in Springer and published over 100 international journal and conference papers. He was awarded a Newton Advanced Fellowship from the Royal Society, UK in 2017. He was a recipient of the IEEE SMC Society Andrew P. Sage Best Transactions Paper Award in 2017. He is serving the Chair of IEEE SMC Society Beijing Capital Region Chapter. He is serving as an Associate Editor of *IEEE Transactions on Neural Networks and Learning Systems*, *IEEE Transactions on Control Systems Technology*, *IEEE Transactions on Systems, Man, and Cybernetics: Systems*, *IEEE/CAA Journal of Automatica Sinica*, *Neurocomputing*, and an Editor of *Journal of Intelligent & Robotic Systems*.

His current research interests include robotics, distributed parameter systems and intelligent control systems.

Long Cheng (SM'14) received the B.S. (Hons.) degree in control engineering from Nankai University, Tianjin, China, in 2004, and the Ph.D. (Hons.) degree in control theory and control engineering from the Institute of Automation, Chinese Academy of Sciences, Beijing, China, in 2009.

He is currently a Full Professor with the Institute of Automation, Chinese Academy of Sciences. He is also an adjunct Professor with University of Chinese Academy of Sciences. He has published over 100 technical papers in peer-refereed journals and prestigious conference proceedings. He was a recipient of the IEEE Transactions on Neural Networks Outstanding Paper Award from IEEE Computational Intelligence Society, the Aharon Katzir Young Investigator Award from International Neural Networks Society and the Young Researcher Award from Asian Pacific Neural Networks Society. He is currently serving as an Associate Editor/Editorial Board Member of IEEE Transactions on Cybernetics, Neural Processing Letters, Neurocomputing, International Journal of Systems Science, and Acta Automatica Sinica.

His current research interests include the rehabilitation robot, intelligent control and neural networks.

Chenguang Yang (M'10-SM'16) is a Professor of Robotics. He received the Ph.D. degree in control engineering from the National University of Singapore, Singapore, in 2010 and performed post-doctoral research in human robotics at Imperial College London, London, UK from 2009 to 2010. He has been awarded EU Marie Curie International Incoming Fellowship, UK EPSRC UKRI Innovation Fellowship, and the Best Paper Award of the IEEE Transactions on Robotics as well as over ten conference Best Paper Awards. His research interest lies in human robot interaction and intelligent system design.

Okyay Kaynak received the B.Sc. degree with first class honors and Ph.D. degrees in electronic and electrical engineering from the University of Birmingham, UK, in 1969 and 1972 respectively. From 1972 to 1979, he held various positions within the industry. In 1979, he joined the Department of Electrical and Electronics Engineering, Bogazici University, Istanbul, Turkey, where he is currently a Professor Emeritus, holding the UNESCO Chair on Mechatronics. He is also a 1000 People Plan Professor at University of Science & Technology Beijing, China. He has hold long-term (near to or more than a year) Visiting Professor/Scholar positions at various institutions in Japan, Germany, U.S., Singapore and China. His current research interests are in the fields of intelligent control and mechatronics. He has authored three books, edited five and authored or co-authored more than 400 papers that have appeared in various journals and conference proceedings.

Dr. Kaynak has served as the Editor in Chief of IEEE Trans. on Industrial Informatics and IEEE/ASME Trans. on Mechatronics as well as Co- Editor in Chief of IEEE Trans. on Industrial Electronics. Additionally, he is on the Editorial or Advisory Boards of a number of scholarly journals. He recently received the Chinese Governments Friendship Award and Humboldt Research Prize (both in 2016).

Dr. Kaynak is active in international organizations, has served on many committees of IEEE and was the president of IEEE Industrial Electronics Society during 2002-2003. He was elevated to IEEE fellow status in 2003.

Yu Wang received the B.E. degree in automation from the Beijing Institute of Technology, Beijing, China, in July 2011, and the Ph.D. degree in control theory and control engineering at the State Key Laboratory of Management and Control for Complex Systems, Institute of Automation, Chinese Academy of Sciences, Beijing, in July 2016. He is currently an Associate Professor in the State Key Laboratory of Management and Control for Complex Systems, Institute of Automation, Chinese Academy of Sciences. His research interests include intelligent control, robotics, and biomimetic robots.